Supporting Information
for

Combination Drug Release of Smart Cyclodextrin-Gated Mesoporous Silica Nanovehicles

Shengwang Zhou,[a] Huizi Sha,[b] Xiaokang Ke,[a] Baorui Liu,[b] Xizhang Wang[a] and Xuezhong Du*[a]

[a] Key Laboratory of Mesoscopic Chemistry (Ministry of Education), State Key Laboratory of Coordination Chemistry, School of Chemistry and Chemical Engineering, Nanjing University, Nanjing 210093, China
[b] The Comprehensive Cancer Center of Drum-Tower Hospital, Medical School of Nanjing University & Clinical Cancer Institute of Nanjing University, Nanjing 210008, China

E-mail: xzdu@nju.edu.cn

Experimental Section

Materials. *N*-Hydroxybenzotriazole (HOBt, 97%), 3-isocyanatopropyltriethoxysilane (95%), 2,3-butanediol (BDO, 97%), cystamine dihydrochloride (97%), and (S)-(+)-camptothecin (CPT, 97%) were purchased from TCI (Shanghai, China), and doxorubicin hydrochloride (DOX) was from Meilun Biology Co. (Dalian, China). L-Glutathione (GSH, 98%), 3-(4,5-dimethylthiazol-2-yl)-2,5-diphenyltetrazolium bromide (MTT, 98%), and tetraethylorthosilicate (TEOS, 99%) were obtained from Sigma-Aldrich. 3-Carboxyphenylboronic acid (99%), 2,2-dimethyl-1,3-propanediol (99%), 1-ethyl-3-(3-dimethyllaminopropyl) carbodiimide hydrochloride (EDC, 98.5%), calcein, rhodamine 6G (Rh6G), dithiothreitol (DTT, 99%), 1,8-octanediamine (ODA, 98%), diethanolamine (99%), 1,2-ethanedithiol (EDT, 97%), γ-cyclodextrin (γ-CD, 98%), and *N*-(2-hydroxyethyl)piperazine-*N*′-(2-ethanesulfonic acid) (HEPES, 99.5%) were purchased from Aladdin (China). The other reagents used in the experiments were acquired from Nanjing Chemical Reagent Co. (China). All of the chemicals used were of analytical grade, and double-distilled water was used.

Synthesis of 2-(3-Carboxyphenyl)-5,5-Dimethyl-1,3,2-Dioxaborinane (1)

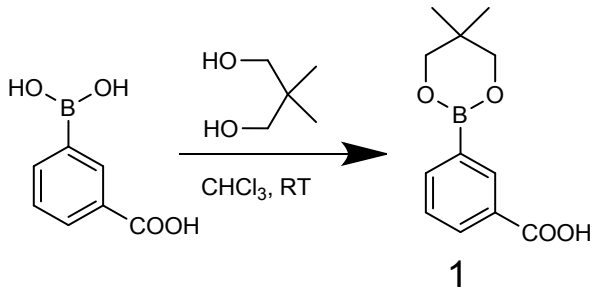

1

To a solution of 3-carboxyphenylboronic acid (1.00 g, 6.00 mmol) in 65 mL of anhydrous chloroform was added 2,2-dimethyl-1,3-propanediol (0.62 g, 6.00 mmol). After stirring for 12 h at 25 °C, the solution mixture was washed with double-distilled water. The organic phase was collected and evaporated under vacuum to obtain **1** (1.35 g, 5.76 mmol, 96%). ^{1}H NMR (500 MHz, $CDCl_3$): δ 8.58 (s, 1H, H-2 phenyl), 8.19 (d, 1H, J = 7.7 Hz, H-4 phenyl), 8.06 (d, 1H, J = 7.3 Hz, H-6 phenyl), 7.49 (t, 1H, J = 7.5 Hz, H-5 phenyl), 3.82 (s, 4H, CH_2), 1.06 (s, 6H, CH_3).

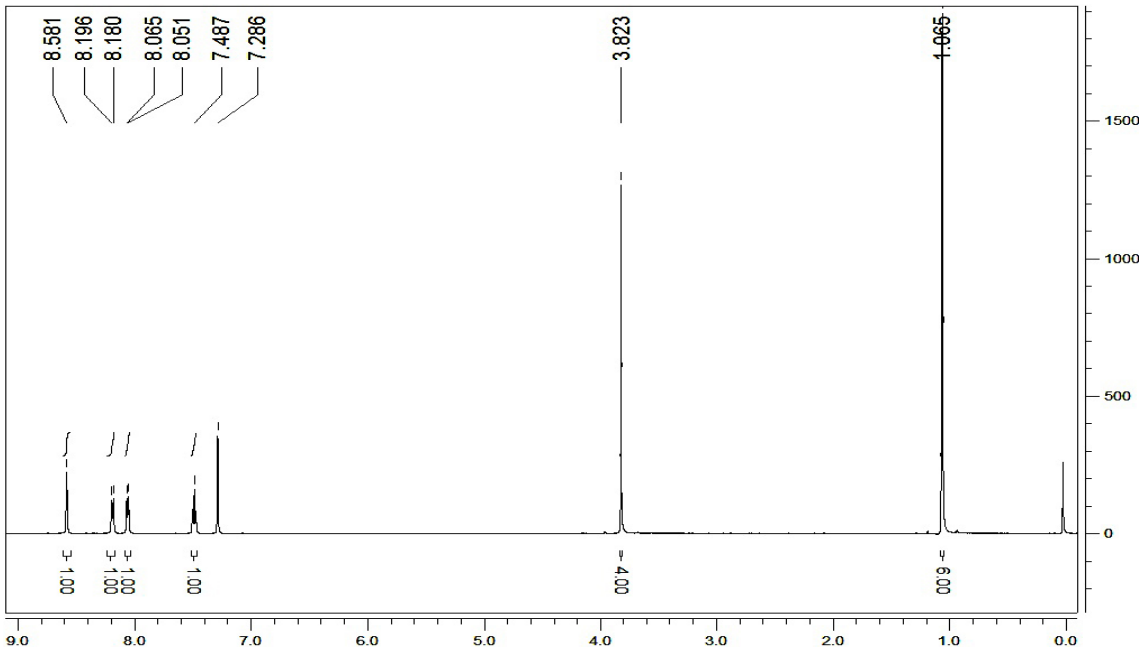

^{1}H NMR spectrum of **1** in $CDCl_3$

Synthesis of *N*-(2-(2-(2-Aminoethyl)disulfanyl)ethyl)-3-(5,5-Dimethyl-1,3,2-dioxaborinan-2-yl)benzamide (2)

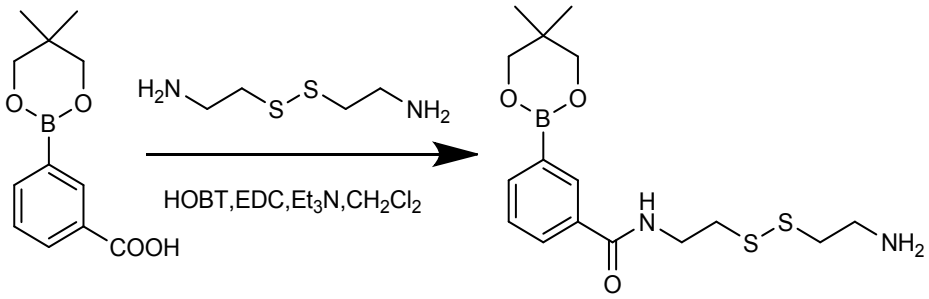

2

1 (0.47 g, 2.00 mmol) was dissolved in 15 mL of anhydrous dichloromethane. To the solution was successively added *N*-hydroxybenzotriazole (0.30 g, 2.20 mmol), 1-ethyl-3-(3-dimethyllaminopropyl)carbodiimide hydrochloride (0.42 g, 2.20 mmol), and triethylamine (0.40 g, 4.00 mmol). The solution mixture was stirred at 25 °C for 12 h, and then, cystamine (0.34 g, 2.2 mmol) was added. The reaction was allowed to proceed for 24 h, and then, the solvent was evaporated under vacuum. The residue was redissolved in saturated NaCl solution and extracted with ethyl acetate. The organic phase was evaporated under vacuum to get a crude product. Purification was carried on by column chromatography to obtain the pure product **2** (0.51 g, 1.38 mmol, 69%). TLC: dichloromethane/methanol, 1:5, v/v. ^{1}H NMR (500 MHz, DMSO-d_6): δ 8.19 (s, 1H, H-2 phenyl), 7.93 (d, 1H, J = 7.6 Hz, H-4 phenyl), 7.83 (d, 1H, J = 7.2 Hz, H-6 phenyl), 7.44 (t, 1H, J = 7.6 Hz, H-5 phenyl), 3.78 (s, 4H, –O–CH_2–), 3.57 (m, 2H, J = 5.8 Hz, –NH–CH_2–), 3.14 (m, 4H, J = 4.5 Hz, –S–CH_2–), 2.95 (m, 2H, J = 6.5 Hz, –CH_2–NH_2), 0.97 (s, 6H, CH_3).

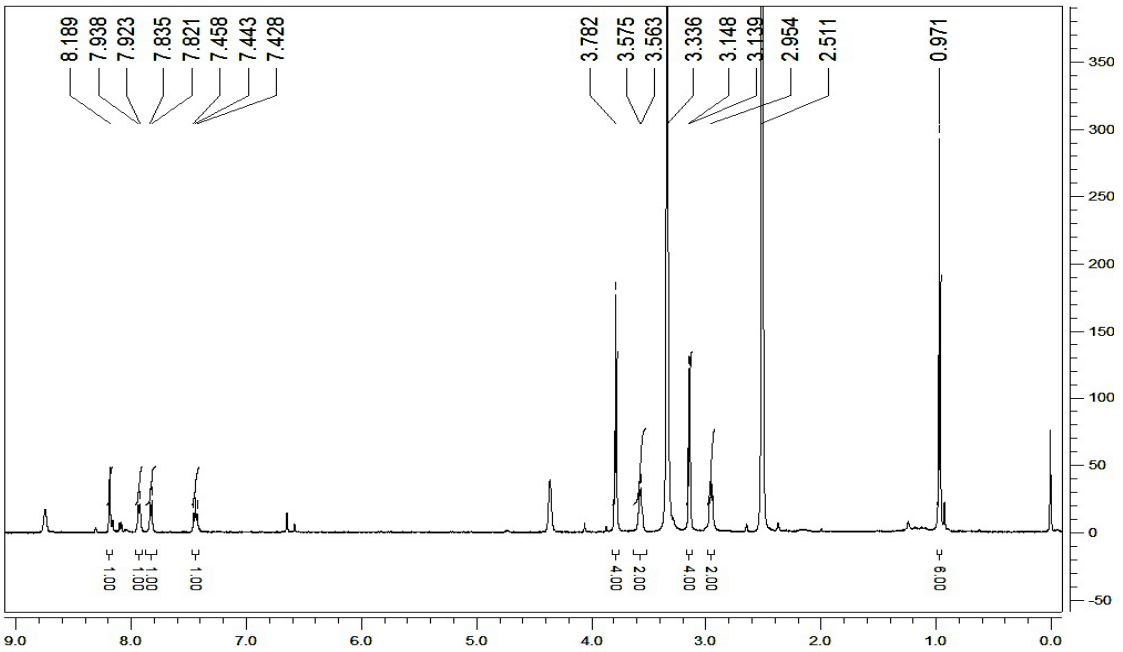

^{1}H NMR spectrum of **2** in DMSO-d_6

Instruments and Measurements. SEM images were acquired on a Hitachi S-4800 microscope, and TEM images were on a JEM-2100 microscope. Powder small-angle XRD measurements were carried out with a Philips X'Pert Prx diffractometer using a Cu-Kα radiation (λ = 0.15405 nm). The surface area, cumulative pore volume, and pore size distribution of MSNs were determined from nitrogen adsorption–desorption isotherms measured on a Micromeritics ASAP2020 porosimeter at 77 K. Thermogravimetric analyses were performed on a Netzsch STA449 F3 thermal analyzer with a heating rate of 10 °C per minute from room temperature to 1000 °C. FTIR spectra were recorded on a Bruker VECTORTM22 spectrometer, UV-vis spectra were on a Shimadzu UV-3600 spectrophotometer, and fluorescence spectra were on a Shimadzu RF-5301PC spectrofluorophotometer. Solid-state NMR spectra were collected on a Bruker Avance400 NMR spectrometer (400 MHz). Hydrodynamic size distributions of MSNs were determined by dynamic light scattering using a 90Plus particle size analyzer (Brookhaven Instruments Co.), and zeta potentials were measured on a zeta potential analyzer (ZetaPALS, Brookhaven Instruments Co.). MTT assays were carried out on a Multiskan Spectrum Microplate Reader (Thermo, USA), and CLSM images were acquired on a confocal laser scanning microscope (CLSM) (Zeiss LSM 710, Germany).

Synthesis of MCM-41-type MSNs. MCM-41 was prepared according to the base-catalyzed sol-gel method. To a solution of cetyltrimethylammonium bromide (CTAB, 0.50 g, 1.37 mmol) in double-distilled water (240 mL) was added aqueous NaOH solution (2 M, 1.75 mL). The solution mixture was then heated to 80 °C. TEOS (2.50 mL, 11.20 mmol) was added dropwise to the solution mixture under vigorous stirring. The suspension was allowed to react for 2 h, and then, the solid precipitate was quickly filtered, washed with distilled water and methanol, and dried in vacuum for 12 h. Afterward, the as-synthesized nanoparticles (0.75 g) were refluxed in a solution mixture of hydrochloride (4.50 mL, 12 M) and methanol (80 mL) at 80 °C for 24 h to remove the CTAB templates. MCM-41-type MSNs were obtained by filtration, washed copiously with methanol, and dried in vacuum at 60 °C.

Preparation of Dioxaborinan Benzamide/Amino-Functionalized MSNs. MCM-41 (0.15 g) was dispersed in 10 mL of anhydrous toluene, and then 3-isocyanatopropyltriethoxysilane (0.60 g, 2.40 mmol) was added followed by stirring at 25 °C for 12 h. Subsequently, compound **2** (0.44 g, 1.20 mmol) was added to the solution mixture followed by refluxing at 90 °C in a nitrogen atmosphere for 6 h. Finally, ODA (0.17 g, 1.20 mmol) was added to the mixture to react under reflux for another 12 h. The dioxaborinan benzamide/amino-functionalized MSNs were collected by centrifugation, washed thoroughly with toluene and methanol, and dried in vacuum for 12 h. The dioxaborinan benzamide-functionalized MSNs were prepared in the same procedure without addition of ODA.

Preparation of PBA/Amino-Functionalized MSNs. The dioxaborinan benzamide/amino-functionalized MSNs (0.15 g) were suspended in 10 mL of isopropanol, and diethanolamine (0.11 g, 1.00 mmol) was added followed by stirring first at 0 °C for 1 h and then at 25 °C for 5 h. The solid nanoparticles were collected by centrifugation followed by redispersing in 10 mL of aqueous sulfuric acid solution (5 mM). The mixture was stirred at 0 °C for 30 min. The PBA/amino-functionalized MSNs (PBA/NH_2-MSNs) were obtained by centrifugation, washing with aqueous ammonia solution (5 mM), double-distilled water, and diethyl ether, and drying in vacuum for 12 h.

Preparation of γ-CD-Gated MSNs with Dual Loading of Calcein and DOX. The aqueous solutions of calcein (0.025 g, 0.4 mM) and DOX (0.058 g, 1 mM) were prepared in 100 mL of HEPES solutions (10 mM, pH 7.4), respectively. PBA/NH_2-MSNs (30 mg) were suspended in 10 mL of aqueous calcein solution (0.4 mM). The suspension was sonicated for the dispersion of the nanoparticles. The mixture was then stirred at 25 °C for 24 h to allow calcein to diffuse into the MSN pores. After addition of γ-CD (130 mg, 0.10 mmol), the suspension was continuously stirred for another 24 h to allow γ-CD to bind the PBA moieties. The solid nanoparticles were collected by centrifugation and then resuspended in 10 mL of aqueous DOX solution (1 mM) followed by stirring for additional 24 h. The drug-loaded nanoparticles were centrifuged and then washed thoroughly with HEPES solution to remove excess cargo and γ-CD from the MSN surfaces. The resulting precipitate was collected by centrifugation and dried in vacuum to get γ-CD-gated MSNs with dual drug loading.

Preparation of γ-CD-Gated MSNs with Dual Loading of Rh6G and CPT. The aqueous Rh6G solution (0.024 g, 0.5 mM) was prepared in 100 mL of HEPES solution (10 mM, pH 7.4), and the aqueous CPT solution (0.035 g, 1 mM) was prepared in a solution mixture of HEPES buffer (95 mL, pH 7.4) and dimethyl sulfoxide (DMSO, 5 mL). The γ-CD-gated MSNs with dual loading of Rh6G and CPT were prepared according to the above procedure.

Controlled Release of Dual Drugs. UV-Vis spectrophotometer was used to monitor the release of Rh6G and CPT. The γ-CD-gated MSNs with dual drug loading (3 mg) were placed in the corner of a 10-mL volumetric flask. HEPES solution (10 mL) was added to the flask slowly to avoid interference with the solid sample. The supernatant was monitored at two absorption maxima (Rh6G, A_{max} = 527 nm; CPT, A_{max} = 355 nm). Fluorescence spectrophotometer was used to monitor the release of calcein and DOX. The supernatant was monitored at two different excitation wavelengths (calcein, λ_{ex} = 458 nm and λ_{em} = 510 nm; DOX, λ_{ex} = 480 nm and λ_{em} = 555 nm). The pH-triggered controlled release was carried out by addition of desired amounts of concentrated hydrochloride solution (0.5 M) to the HEPES solution to reach pH 5.0 or 3.0. Additionally, fructose, galactose, or glucose was added to the HEPES solution (pH 7.4) to reach 10 mM for competitive binding-triggered controlled

release. The redox-responsive controlled release was performed by addition of DTT, GSH, or other triggers to the HEPES solution (pH 7.4) to obtain different concentrations.

Preparation of γ-CD-Gated MSNs with Dual Loading of CPT and DOX for in Vitro Cell Assay. PBA/NH_2-MSNs (30 mg) were added to the aqueous CPT solution (1 mM, 10 mL of HEPES solution and DMSO, pH 7.4) under stirring for 24 h to allow the diffusion of CPT into the MSN pores. Afterward, γ-CD (130 mg, 0.10 mmol) was added, and the mixture was continuously stirred for another 24 h for capping of γ-CD. The nanoparticles were centrifuged and then redispersed in the aqueous DOX solution (1 mM, 10 mL of HEPES solution, pH 7.4) followed by stirring for another 24 h. The drug-loaded nanoparticles were centrifuged and then washed copiously with HEPES solution to remove excess drugs and γ-CD from the MSN surfaces. The resulting precipitate was centrifuged and dried in vacuum to get γ-CD-gated MSNs with dual drug loading.

Cell Lines and Cell Culture. Both human cervical carcinoma cell lines HeLa and human lung adenocarcinoma cell lines A549 were purchased from Cell Bank of Shanghai Institute of Biochemistry and Cell Biology (China). The cells were cultured in Dulbecco's modified Eagle's medium (DMEM) containing 10% fetal bovine serum (FBS), 100 U/mL penicillin, and 100 μg/ml streptomycin (Invitrogen, Grand Island, NY, USA). The cultures were maintained in a 5% CO_2 humidified atmosphere at 37 °C.

In Vitro Cytotoxicity Assay. The in vitro cell viability was detected by the 3-(4,5-dimethylthiazol-2-yl)-2,5-diphenyltetrazolium bromide (MTT) assay. HeLa and A549 cells were used to test the cytotoxicity of the γ-CD-gated MSNs with and without CPT and DOX loading. The cells were seeded into a 96-well cell culture plate at a density of 8×10^3 cells per well for 12 h of incubation. The γ-CD-gated MSNs with and without CPT and DOX loading were introduced with different concentrations of 12.5, 25, 50, 100, 200, and 400 μg/mL. After 24 h of incubation, the culture media were removed, and the cells were continuously treated with 0.5 mg/mL MTT solution for 4 h. After that, the supernatant was removed, and the precipitated formazan was dissolved by adding 100 μL of DMSO to each well. The absorbance of each well was measured at 570 nm using a Multiskan spectrum microplate reader (Thermo, USA).

CLSM Images of Intracellular Drug Release. HeLa and A549 cells were seeded and cultured using the above method. The γ-CD-gated MSNs with dual loading of CPT and DOX were added to each well with a final concentration of 100 μg/mL, and the intracellular drug release behaviors after different incubation times (3, 6, 12, and 24 h) were visualized using CLSM. The CLSM images were acquired in different optical windows for CPT (λ_{ex} = 365 nm, blue color) and DOX (λ_{ex} = 488 nm, red color).

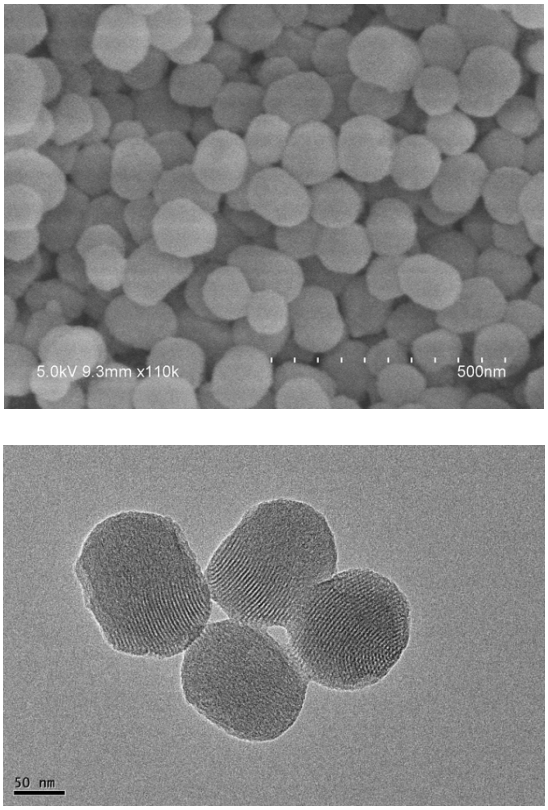

Fig. S1 SEM (top) and TEM (bottom) images of MCM-41 nanoparticles.

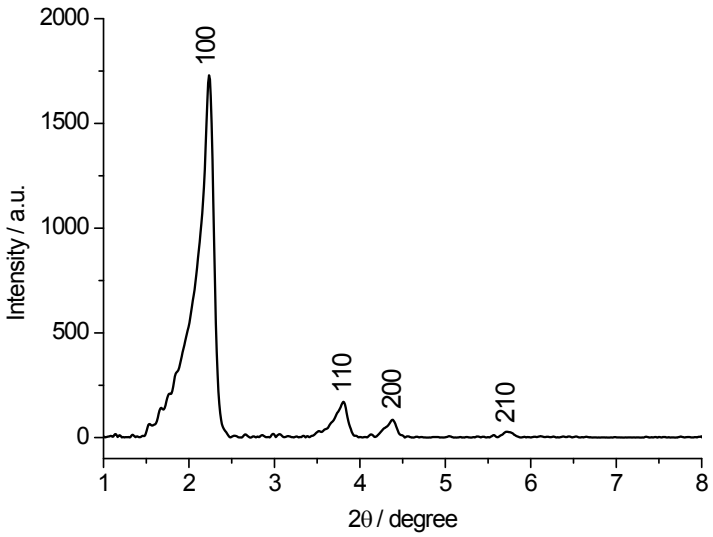

Fig. S2 Small-angle powder XRD patterns of MCM-41 nanoparticles.

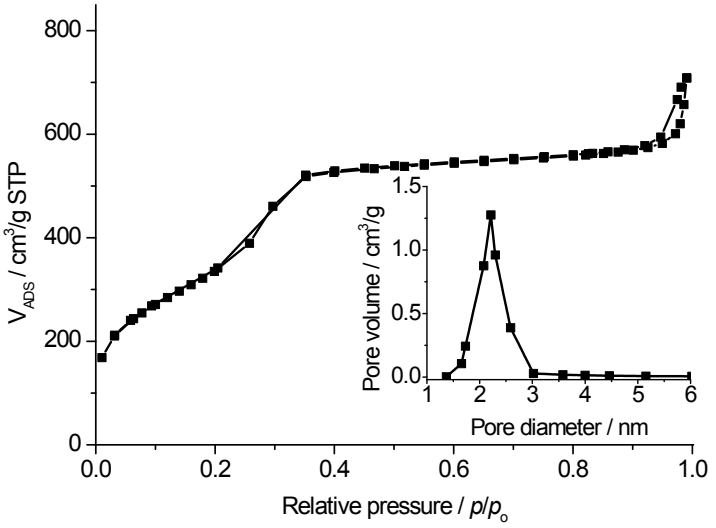

Fig. S3 Nitrogen adsorption–desorption isotherms of MCM-41 nanoparticles. Inset shows pore size distribution.

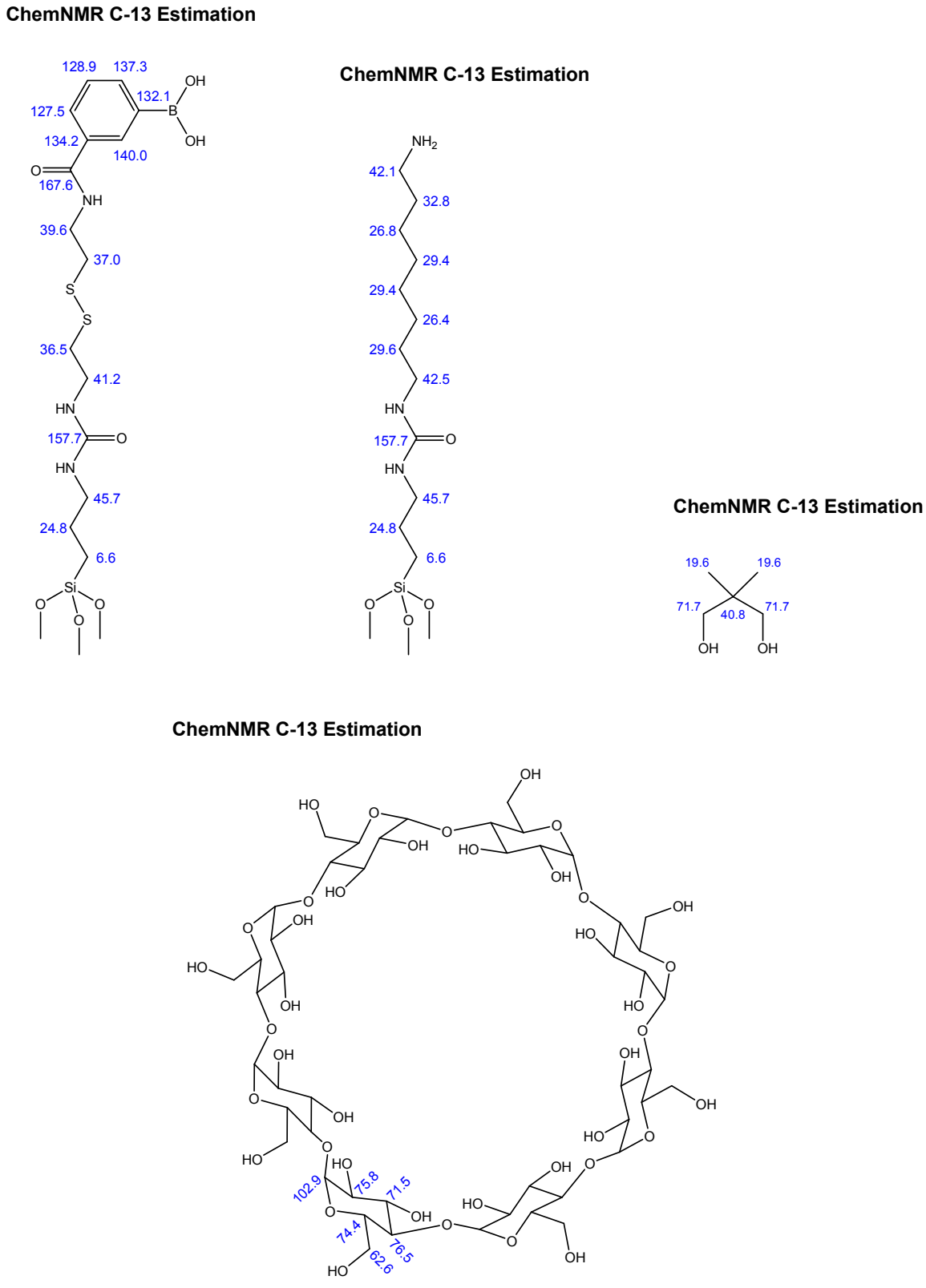

Fig. S4 Predicted ^{13}C NMR chemical shifts (ppm) of relevant materials from ChemDraw Ultra 8.0 for the references of the resonances of ^{13}C NMR spectra.

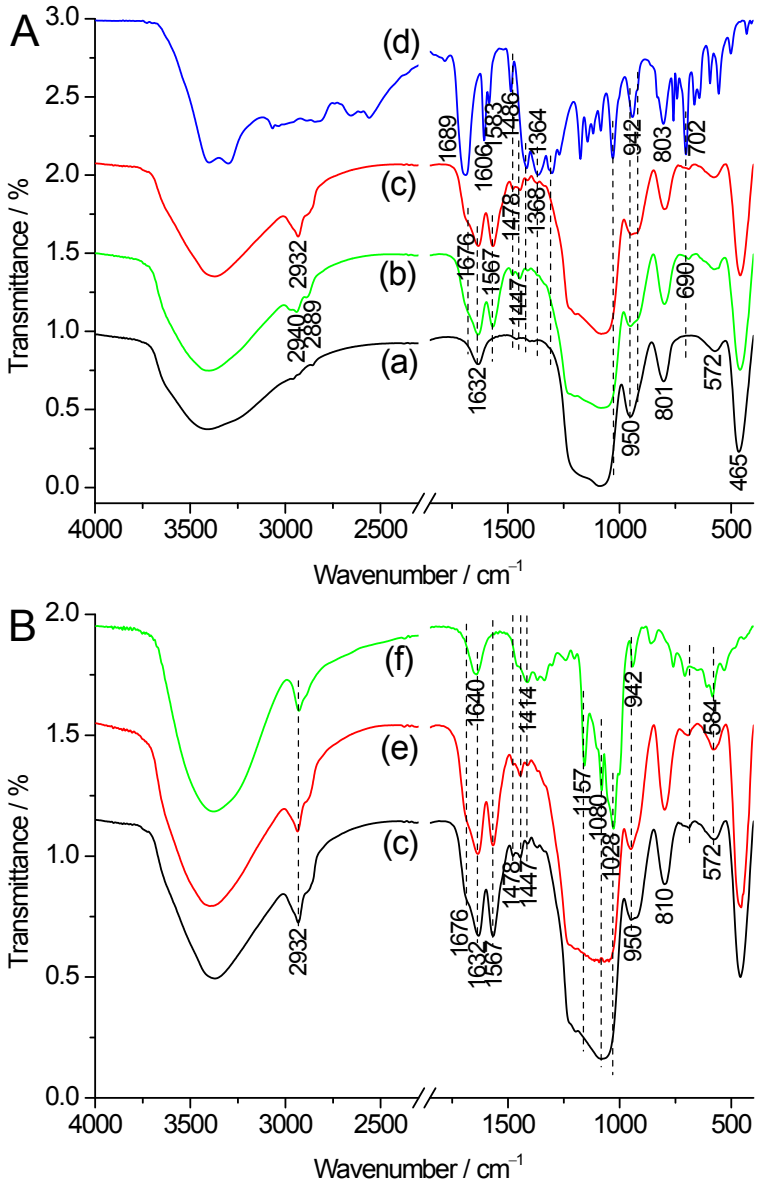

Fig. S5 FTIR spectra of (a) MCM-41, (b) PBA-MSNs, (c) PBA/NH_2-MSNs, (d) 3-carboxyphenylboronic acid, (e) γ-CD-gated MSNs, and (f) γ-CD.

FTIR spectroscopy was used to characterize the modification of the PBA moieties and amines. After MCM-41 was modified with the disulfide-linked carbamoylphenylboronic acid moieties, the strong bands at 1676 and 1567 cm^{-1} were assigned to the amide I and amide II bands of the –NHCONH– linkages, respectively, and the bands at 1478 and 1447 cm^{-1} were attributed to the skeletal stretching vibrations of phenyl groups mixed with the CH_2 bending vibrations. At the same time, the intensity of the band at 950 cm^{-1} related to silanols was decreased to some degree. After the further modification of 1,8-octanediamine (ODA), the band at 2932 cm^{-1}, due to the CH_2 stretching vibrations, was obviously intensified. After subsequent capping with γ-CD, the band at 1445 cm^{-1} due to CH_2 bending vibrations was increased in intensity; however, the bands around 1050–1200 cm^{-1} related to the various C–O stretching vibrations could not be unambiguously distinguished, because the bands were overlapped with the strong Si–O–Si stretching bands of silica matrix at 1000–1230 cm^{-1}.

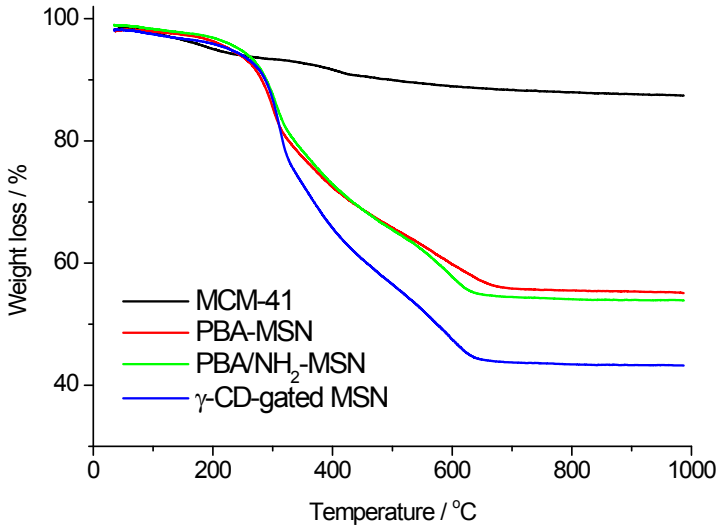

Fig. S6 Thermogravimetric analysis profiles of MCM-41, PBA-MSNs, PBA/NH_2-MSNs, and γ-CD-gated MSNs without drug loading.

The surface densities of the PBA moieties and amino groups were determined to be 1.290 and 0.345 mmol/g MCM-41 by thermogravimetric analysis, respectively, and the amount of bound γ-CD was determined to be 0.302 mmol/g MCM-41 (without drug loading).

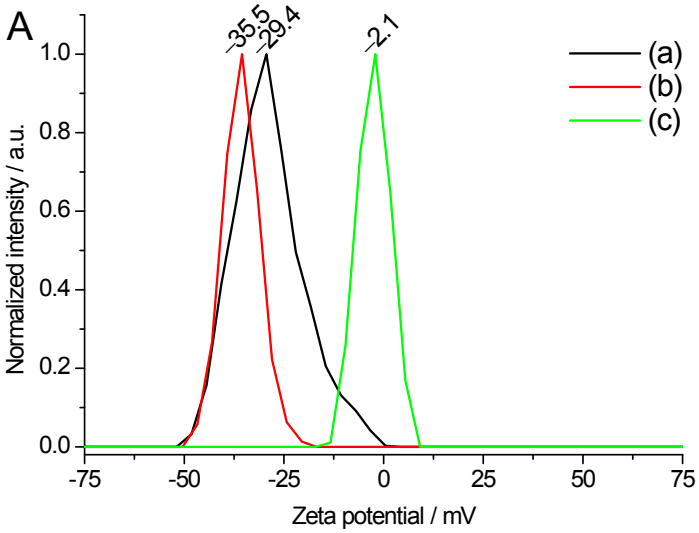
A
-35.5
-29.4
-2.1
(a)
(b)
(c)
Normalized intensity / a.u.
Zeta potential / mV

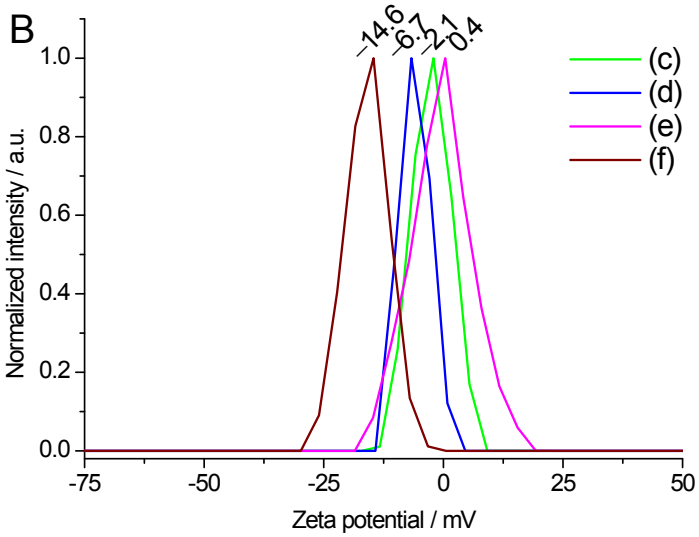
B
-14.6
-6.7
-2.1
0.4
(c)
(d)
(e)
(f)
Normalized intensity / a.u.
Zeta potential / mV

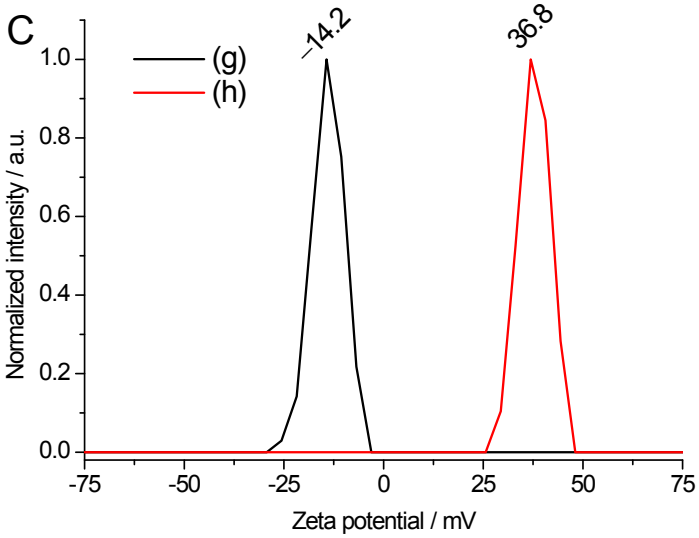
C
-14.2
36.8
(g)
(h)
Normalized intensity / a.u.
Zeta potential / mV

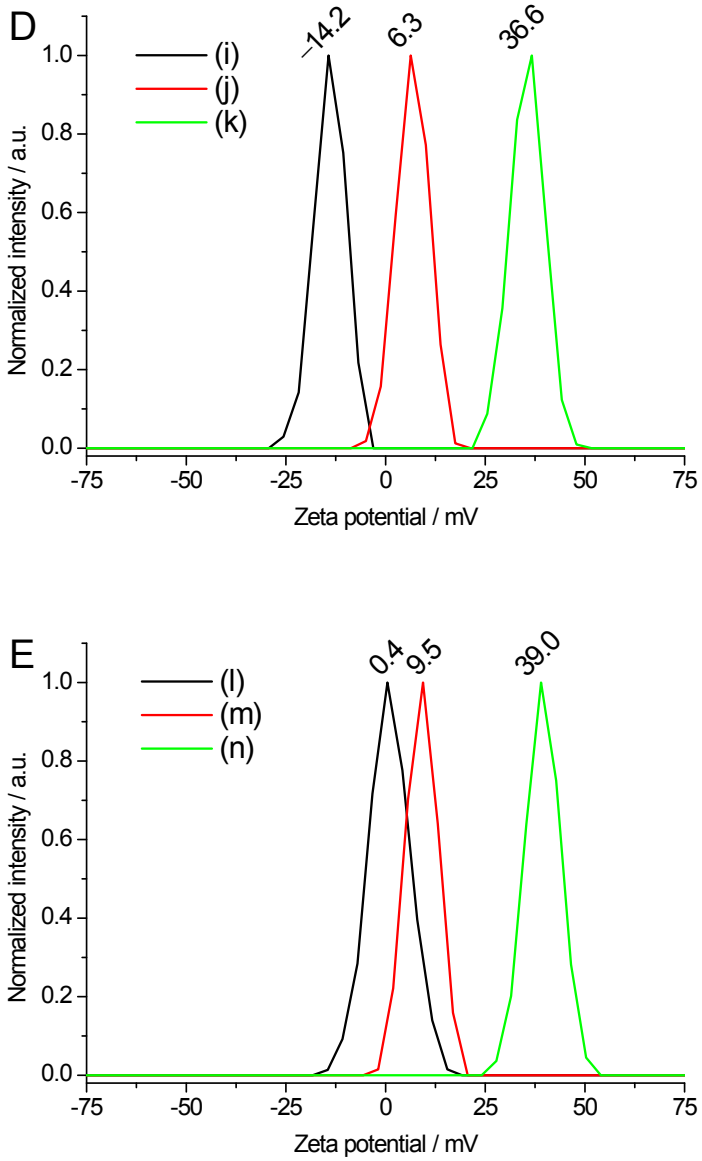

Fig. S7 (A,B) Zeta potentials of (a) MCM-41, (b) PBA-MSNs, (c) PBA/NH_2-MSNs, (d) γ-CD-gated MSNs without drug loading, (e) γ-CD-gated MSNs with the inclusion of DOX in the γ-CD cavities, and (f) γ-CD-gated MSNs with the inclusion of CPT in the γ-CD cavities at pH 7.4.
(C) Zeta potentials of (g) γ-CD-gated MSNs with dual loading of Rh6G and CPT at pH 7.4 and (h) MSNs after drug release upon trigger of pH 5.0.
(D) Zeta potentials of (i) γ-CD-gated MSNs with dual loading of Rh6G and CPT at pH 7.4, (j) MSNs after Rh6G drug release upon first trigger of fructose (10 mM), and (k) MSNs after CPT release upon subsequent trigger of pH 5.0.
(E) Zeta potentials of (l) γ-CD-gated MSNs with dual loading of calcein and DOX at pH 7.4, (m) MSNs after calcein release upon first trigger of DTT (5 mM), and (n) MSNs after DOX release upon subsequent trigger of pH 5.0.

Irrespective of simultaneous and cascade release of the dual drugs, **the ultimate nanoparticles after release of each drug were in the aqueous solutions at pH 5.0, and their Zeta pontentials were in the range of 36–39 mV** owing to the protonation of the modified amino groups.

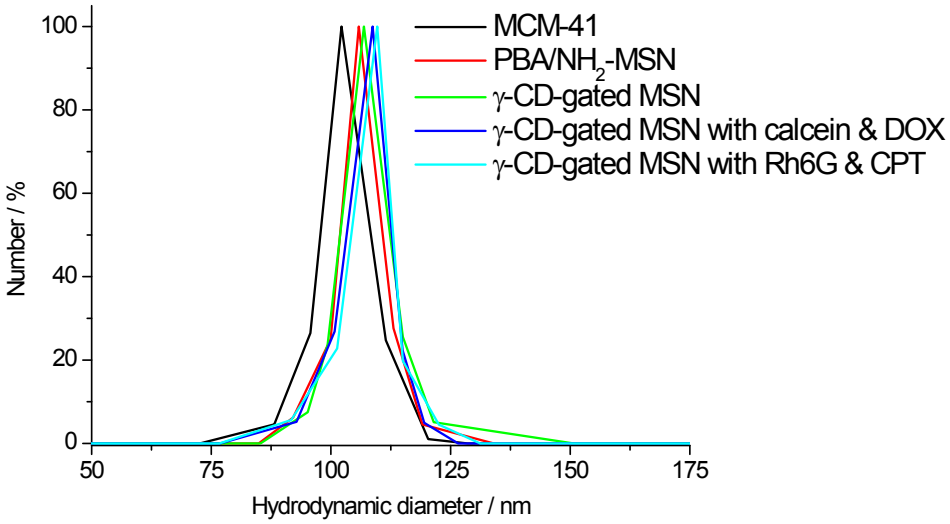

Fig. S8 Hydrodynamic diameter distributions of MCM-41, PBA/NH_2-MSNs, γ-CD-gated MSNs without drug loading, γ-CD-gated MSNs with dual loading of calcein and DOX, and γ-CD-gated MSNs with dual loading of Rh6G and CPT.

The average hydrodynamic diameters of MCM-41, PBA/NH_2-MSNs, the γ-CD-gated MSNs without drug loading, the γ-CD-gated MSNs with dual loading of calcein and DOX, and the γ-CD-gated MSNs with dual loading of Rh6G and CPT were 102, 106, 107, 109, and 110 nm (Fig. S8), respectively. Considering the extended length (ca. 2.0–2.2 nm) of the flexible disulfide-linked chains terminated with the PBA moieties and modified amines on the MSN surface, it is reasonable that the average hydrodynamic diameters after PBA/amino functionalization increased by 4 nm. Taking into account the height of γ-CD (0.79 nm), it is likely that additional increase of 1–2 nm in hydrodynamic diameter upon further binding of γ-CD to PBA/NH_2-MSNs.

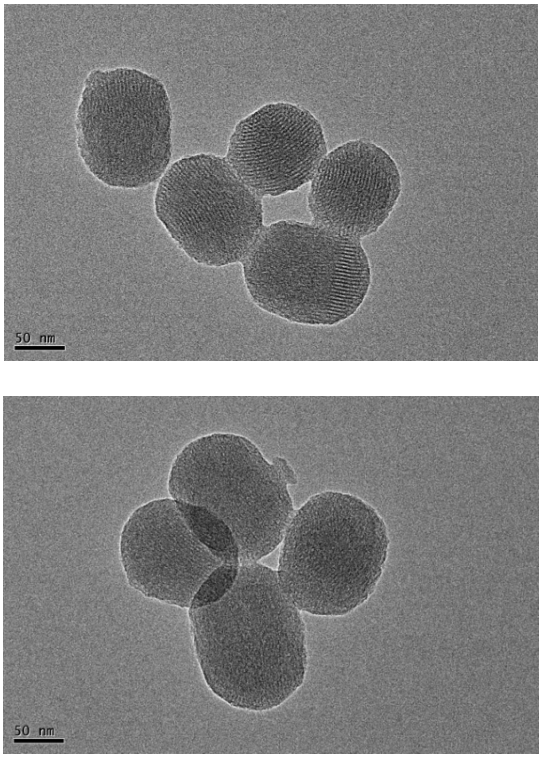

Fig. S9 TEM images of (top) PBA/NH_2-MSNs and (bottom) γ-CD-gated MSNs without drug loading.

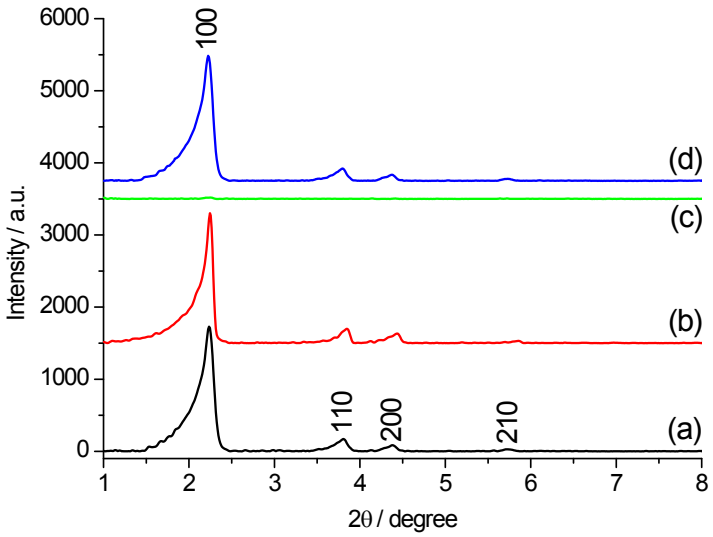

Fig. S10 Small-angle powder XRD patterns of (a) MCM-41, (b) PBA/NH_2-MSNs, and γ-CD-gated MSNs with dual loading of Rh6G and CPT (c) before and (d) after drug release upon trigger of pH 3.0.

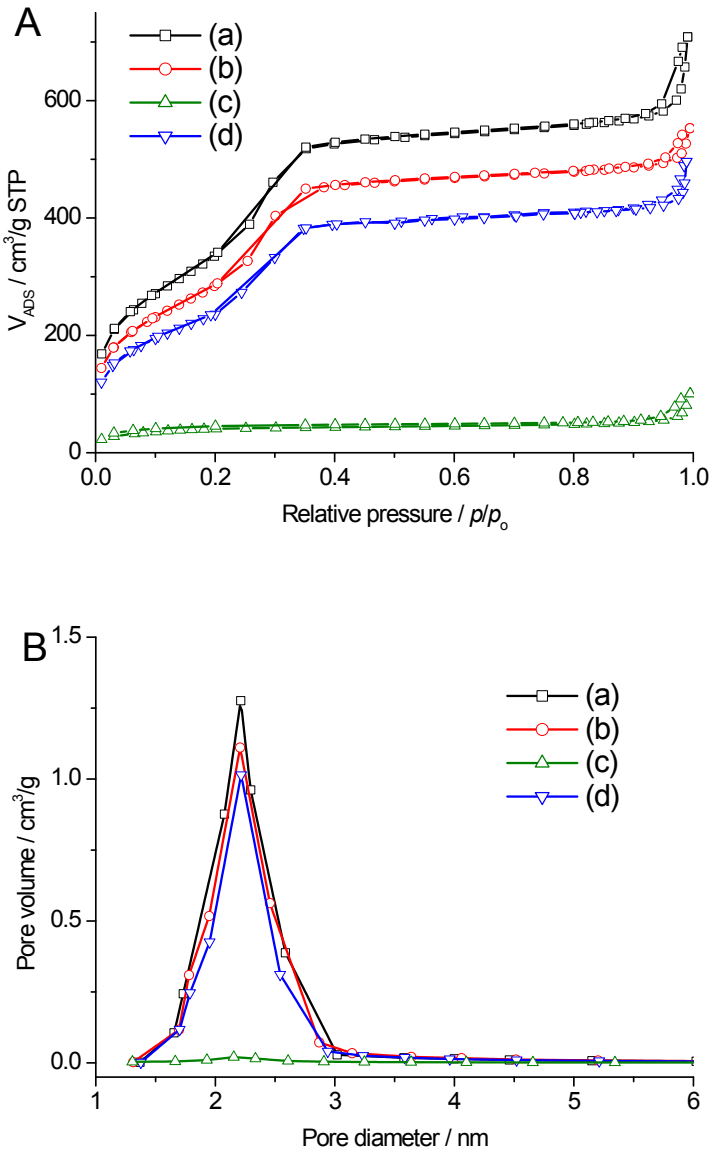

Fig. S11 (A) Nitrogen adsorption–desorption isotherms and (B) pore size distributions of (a) MCM-41, (b) PBA/NH_2-MSNs, and γ-CD-gated MSNs with the loading of Rh6G and CPT (c) before and (d) after drug release upon trigger of pH 3.0.

Table S1. Surface areas and average pore sizes of MSN materials calculated from the nitrogen adsorption–desorption isotherms.

materials	surface area (m^2/g)	pore size (nm)
MCM-41	1133.5	2.2
PBA/NH_2-MSNs	926.3	2.2
γ-CD-gated MSNs with dual loading of Rh6G and CPT	100.8	–
γ-CD-gated MSNs after drug release triggered by pH 3.0	870.9	2.2

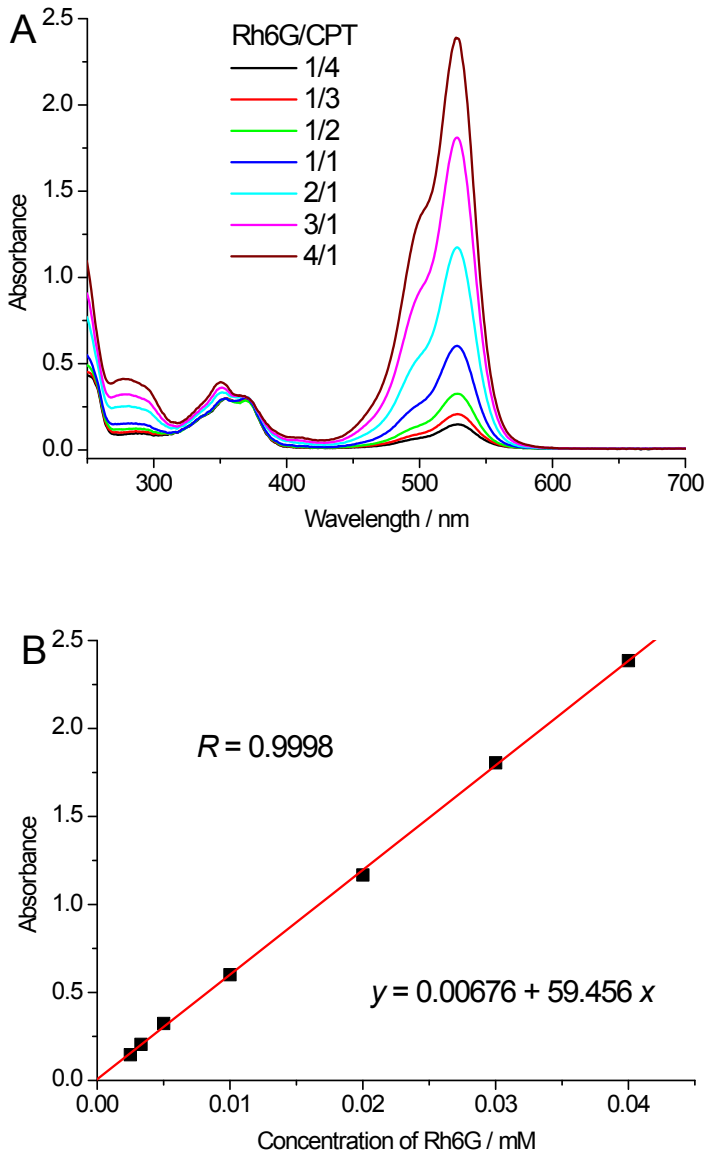

Fig. S12 (A) UV-Vis spectra of the solution mixtures of Rh6G and CPT with different molar ratios when CPT was fixed at 0.01 mM. (B) The absorption intensity at 527 nm as a function of concentration of Rh6G in the solution mixtures.

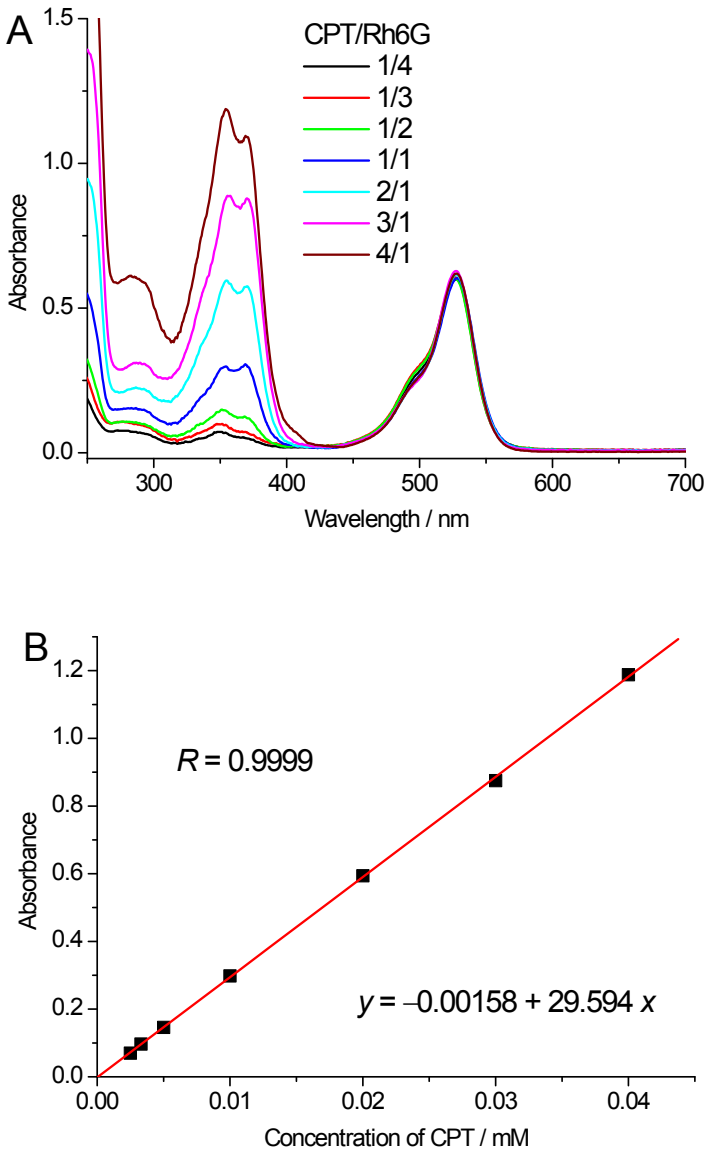

Fig. S13 (A) UV-Vis spectra of the solution mixtures of CPT and Rh6G with different molar ratios when Rh6G was fixed at 0.01 mM. (B) The absorption intensity at 355 nm as a function of concentration of CPT in the solution mixtures.

UV-vis spectroscopy was used to monitor simultaneous release of Rh6G from the MSN pores and CPT from the γ-CD cavities. The maximum absorption bands of Rh6G (A_{max} = 527 nm) and CPT (A_{max} = 355 nm) in their solution mixtures were well resolved. The absorption intensity of one kind of drugs increased linearly with concentration when the other kind of drugs was present at the fixed concentrations with almost unchanged absorption intensities (Fig. S12 and S13). That means that no interference could occur for the monitoring of controlled release of the two drugs.

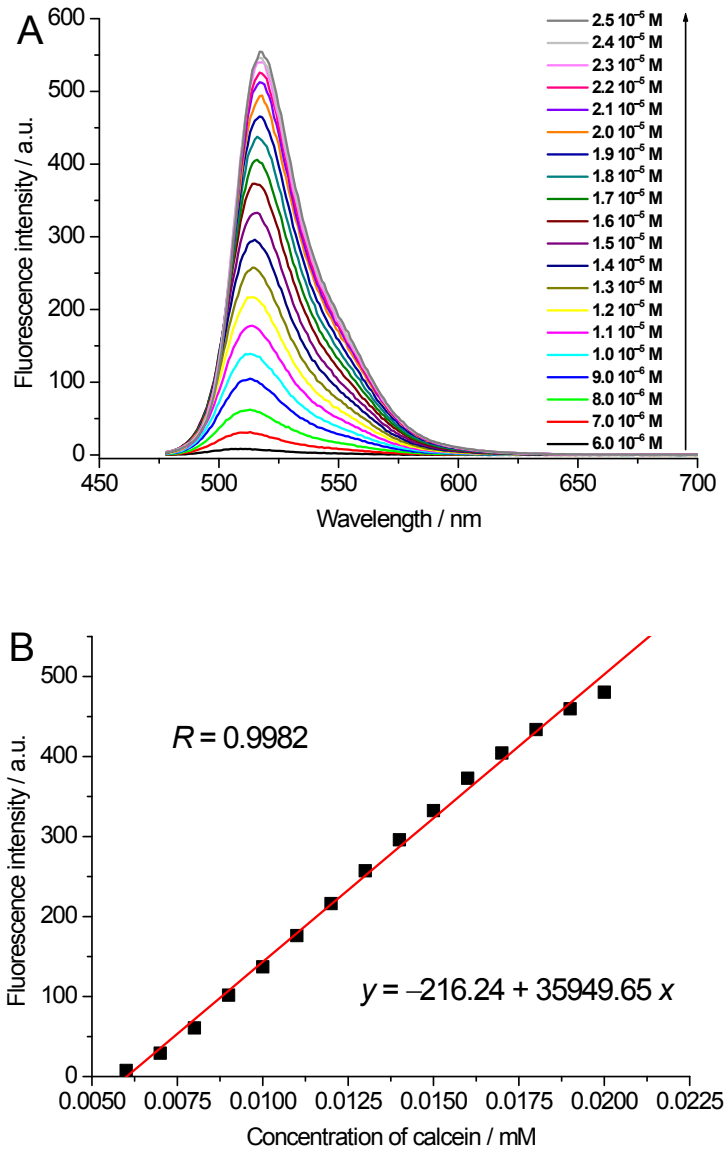

Fig. S14 (A) Fluorescence spectra of aqueous calcein solutions (λ_{ex} = 458 nm, λ_{em} = 510 nm) with different concentrations. (B) Fluorescence intensity at 510 nm as a function of concentration of aqueous calcein solutions.

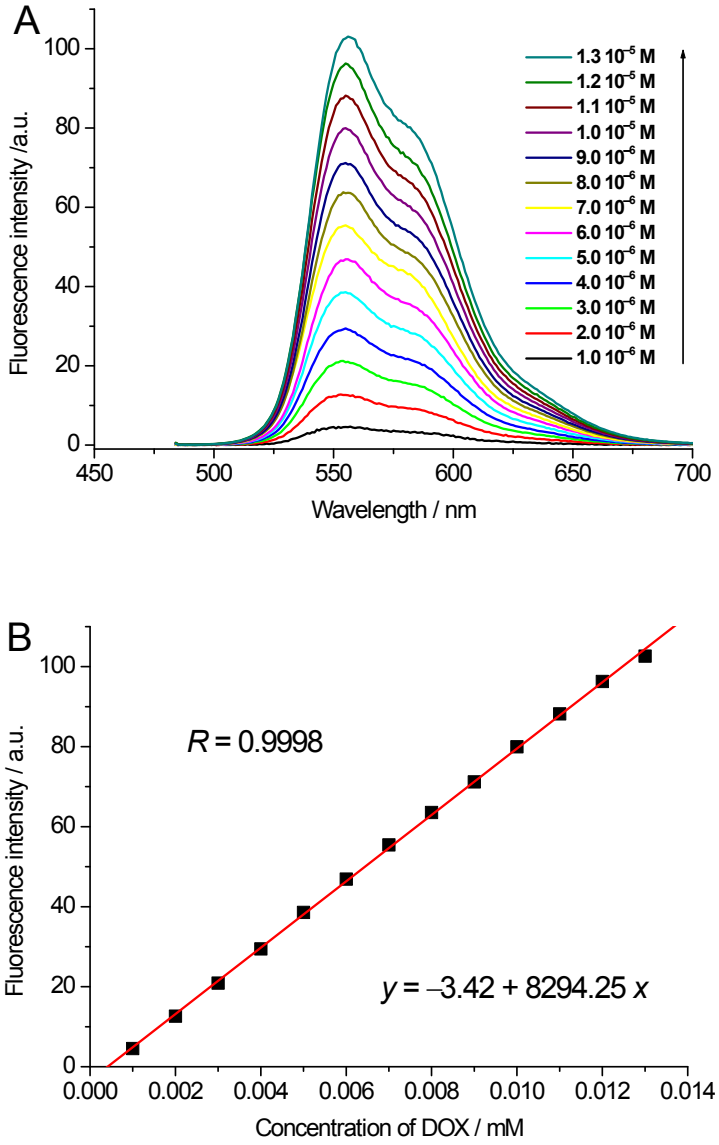

Fig. S15 (A) Fluorescence spectra of aqueous DOX solutions (λ_{ex} = 480 nm, λ_{em} = 555 nm) with different concentrations. (B) Fluorescence intensity at 555 nm as a function of concentration of aqueous DOX solutions.

Fluorescence spectroscopy was used to monitor cascade release of calcein from the MSN pores and DOX from the γ-CD cavities. The fluorescence intensities of aqueous solutions of calcein (λ_{ex} = 458 nm and λ_{em} = 510 nm) and DOX (λ_{ex} = 480 nm and λ_{em} = 555 nm) increased linearly with concentration, respectively (Fig. S14 and S15). It is worth noting that the fluorescence of calcein was almost quenched at acid pH, which suggests that the release of calcein had no influence on monitoring of subsequent release of DOX triggered by acid pH besides a small difference in excitation wavelength.

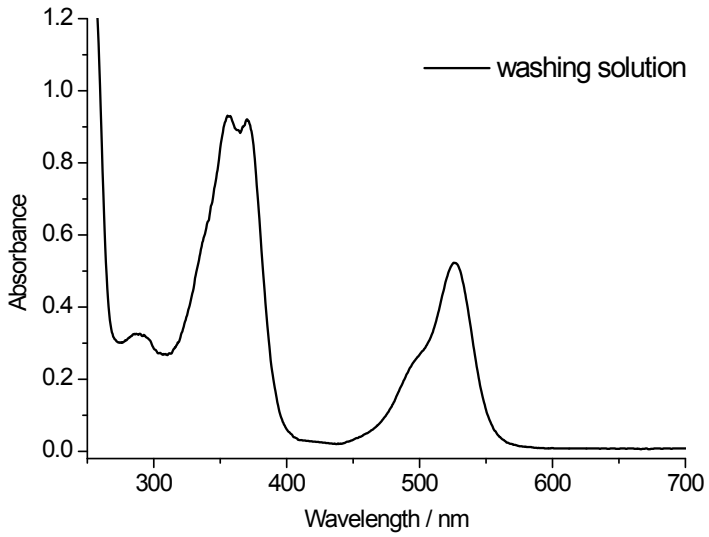

Fig. S16 UV-Vis spectra of the final washing soltion containing unloaded Rh6G and CPT in 250 mL of HEPES solution.

The loading capacities of Rh6G and CPT were carried out as follows. Firstly, 30 mg of PBA/NH_2-MSNs were suspended in of 10 mL of HEPES solution containing Rh6G (0.5 mM) for Rh6G loading. Secondly, γ-CD was added to the suspension for capping of MSN entrances. After 24h of stirring, solid nanoparticles were centrifuged and the supernatant was collected for following UV-vis spectral analysis. Thirdly, 10 mL of aqueous CPT solution (1 mM) was added for CPT loading, followed by centrifugation and washing with HEPES solution to remove excess cargo and γ-CD. Finally, all washing solutions of Rh6G and CPT were collected and diluted to a certain volume. The UV-vis spectra of the final washing solution were measured, and the Rh6G and CPT concentrations of the final washing solution were determined from the standard curves of absorption intensity of aqueous Rh6G and CPT solutions versus concentration (Fig. S12B and S13B), respectively. The difference between the initially added (total) and unloaded (washed) amounts of Rh6G and CPT were calculated to determine the loading capacities of Rh6G encapsulated within the MSN pores and CPT included in the γ-CD cavities. The loading capacities of Rh6G and CPT were determined to be 0.0947 and 0.0707 mmol/g PBA/NH_2-MSN using UV-vis spectroscopy, respectively.

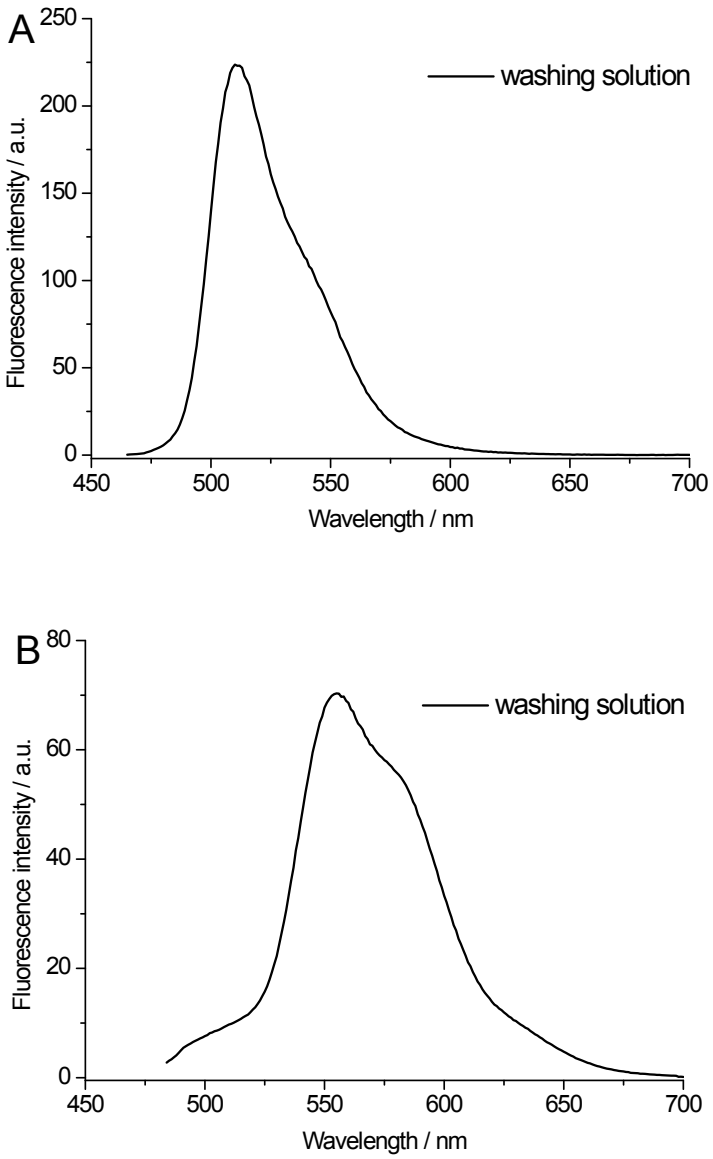

Fig. S17 Fluorescence spectra of final washing solutions containing unloaded (A) calcein (λ_{ex} = 458 nm, λ_{em} = 510 nm) in 250 mL of HEPES solution and (B) DOX (λ_{ex} = 480 nm, λ_{em} = 555 nm) in 1000 mL HEPES solution, respectively.

The loading capacities of calcein and DOX were carried out as follows. Firstly, 30 mg of PBA/NH_2-MSNs were suspended in of 10 mL of HEPES solution containing calcein (0.4 mM) for calcein loading. Secondly, γ-CD was added to the suspension for capping of MSN entrances. After 24h of stirring, solid nanoparticles were centrifuged and the supernatant was collected for following fluorescence spectral analysis. Thirdly, 10 mL of aqueous DOX solution (1 mM) was added for DOX loading, followed by centrifugation and washing with HEPES solution to remove excess cargo and γ-CD. Finally, all washing solutions of calcein and DOX were collected and diluted to a certain volume. The fluorescence spectrum of calcein of the final washing solution was first measured, and the fluorescence spectrum of DOX was then measured after adjustment of pH to 3.0 to quench the fluorescence emission of calcein. The calcein and DOX concentrations of the final washing solution were

determined from the standard curves of fluorescence intensity of aqueous calcein and DOX solutions versus concentration (Fig. S14B and S15B), respectively. The difference between the initially added (total) and unloaded (washed) amounts of calcein and DOX were calculated to determine the loading capacities of calcein encapsulated within the MSN pores and DOX included in the γ-CD cavities. The loading capacities of calcein and DOX were determined to be 0.0316 and 0.0367 mmol/g PBA/NH_2-MSN using fluorescence spectroscopy, respectively.

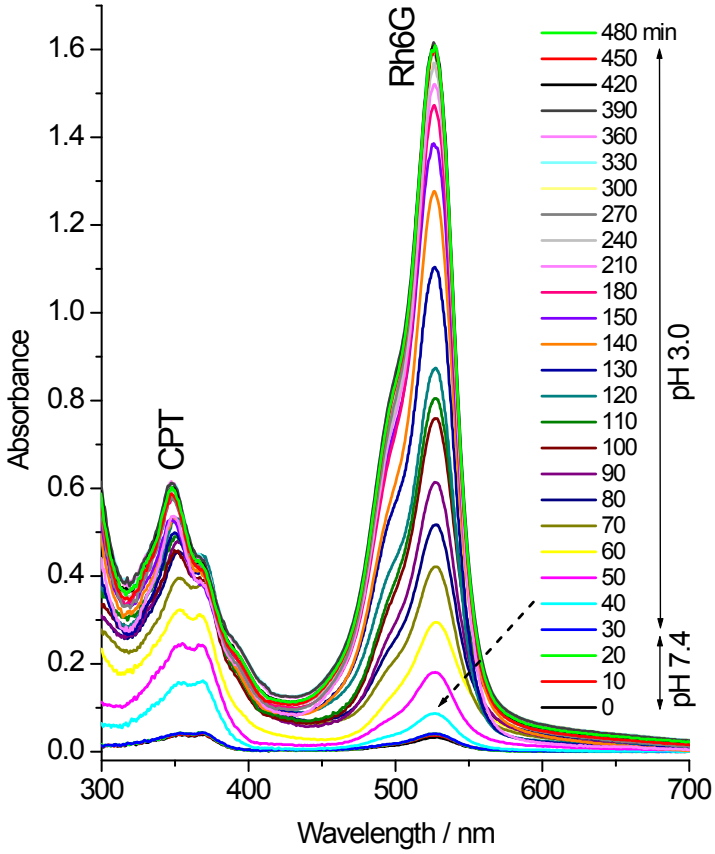

Fig. S18 UV-vis spectra of Rh6G and CPT released from the HEPES solution of γ-CD-gated MSNs with dual loading of Rh6G and CPT upon change of pH from 7.4 to 3.0 after 30 min.

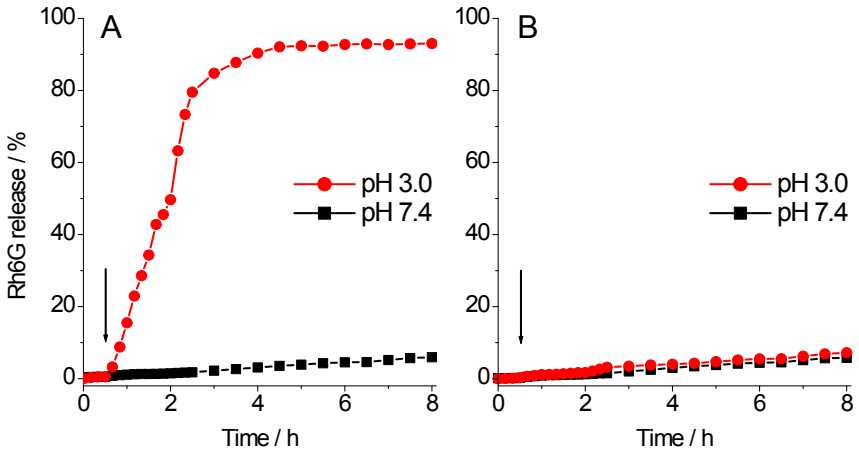

Fig. S19 Comparison of pH-responsive release profiles of Rh6G from (A) γ-CD-gated MSNs only with loading of Rh6G in the MSN pores and (B) PBA-MSNs without modification of ODA after addition of Rh6G and γ-CD (followed by washing) upon change of pH from 7.4 to 3.0 after 30 min. The arrows indicate the change of pH.

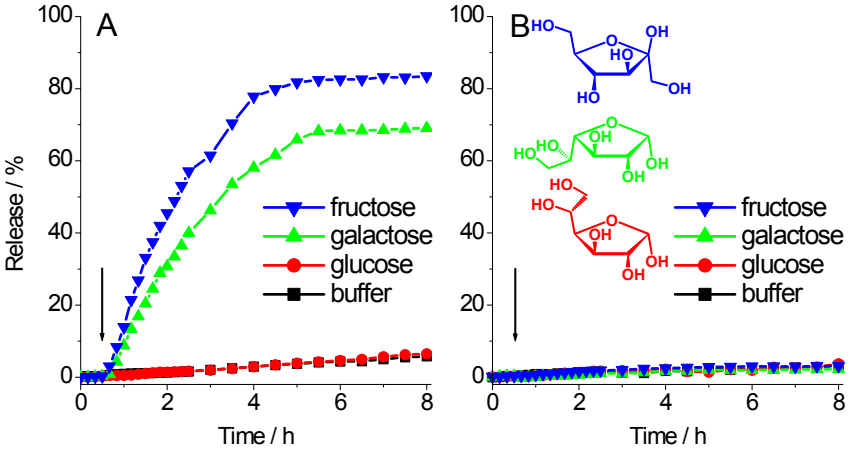

Fig. S20 Saccharide-triggered release profiles from γ-CD-gated MSNs with dual loading of Rh6G and CPT in the HEPES solutions (pH 7.4): (A) Rh6G (A_{max} = 527 nm); (B) CPT (A_{max} = 355 nm). The arrows indicate the addition of saccharides (10 mM).

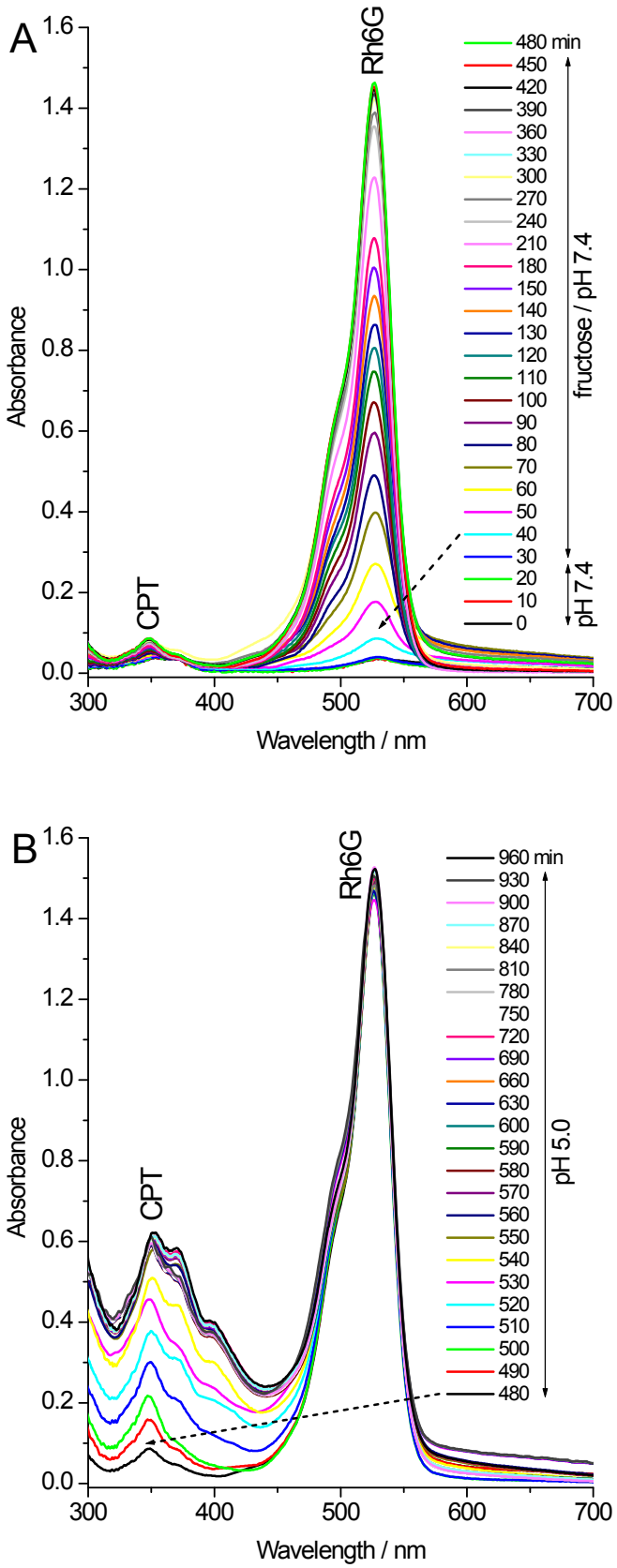

Fig. S21 UV-vis spectra of Rh6G and CPT released from the HEPES solution (pH 7.4) of γ-CD-gated MSNs with dual loading of Rh6G and CPT upon first trigger of fructose (10 mM) after 30 min and subsequent trigger of pH 5.0 after 480 min.

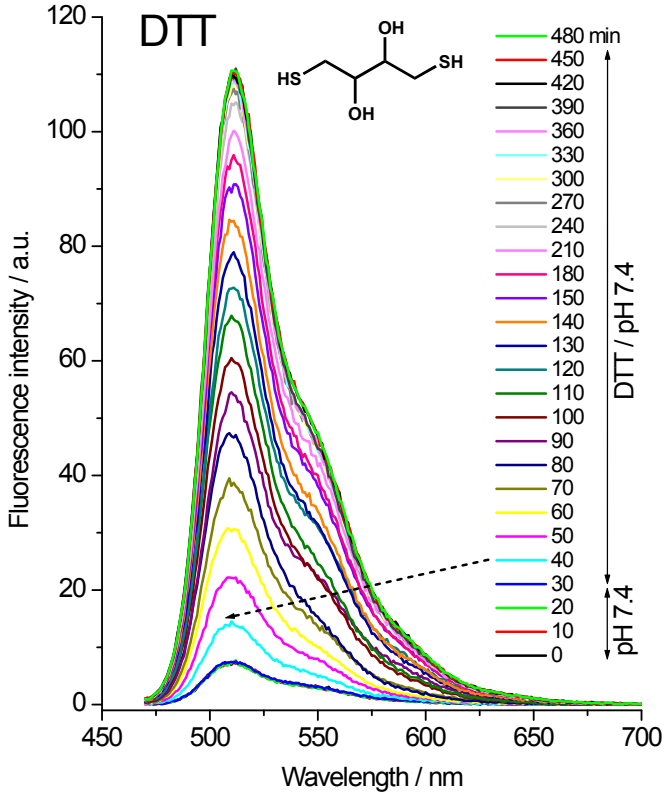

Fig. S22 Fluorescence spectra of calcein (λ_{ex} = 458 nm, λ_{em} = 510 nm) released from γ-CD-gated MSNs with dual loading of calcein and DOX upon trigger of DTT (5 mM) at pH 7.4 after 30 min.

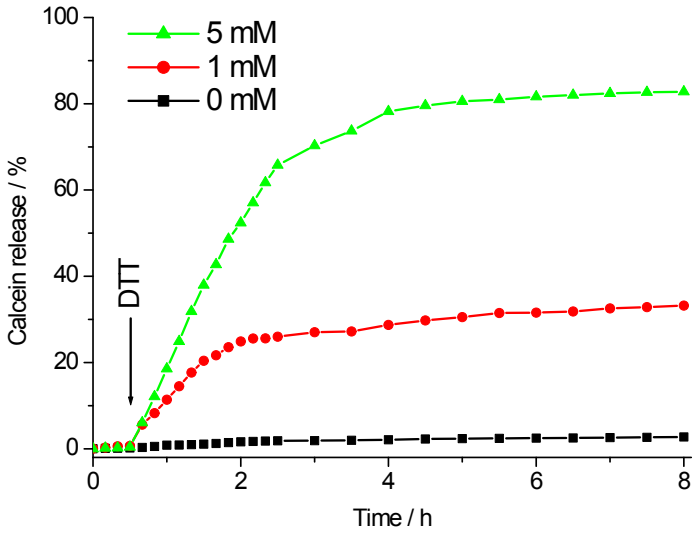

Fig. S23 DTT-responsive release profiles of calcein (λ_{ex} = 458 nm, λ_{em} = 510 nm) from γ-CD-gated MSNs with dual loading of calcein and DOX with different concentrations of DTT at pH 7.0. The arrow indicate the addition of DTT.

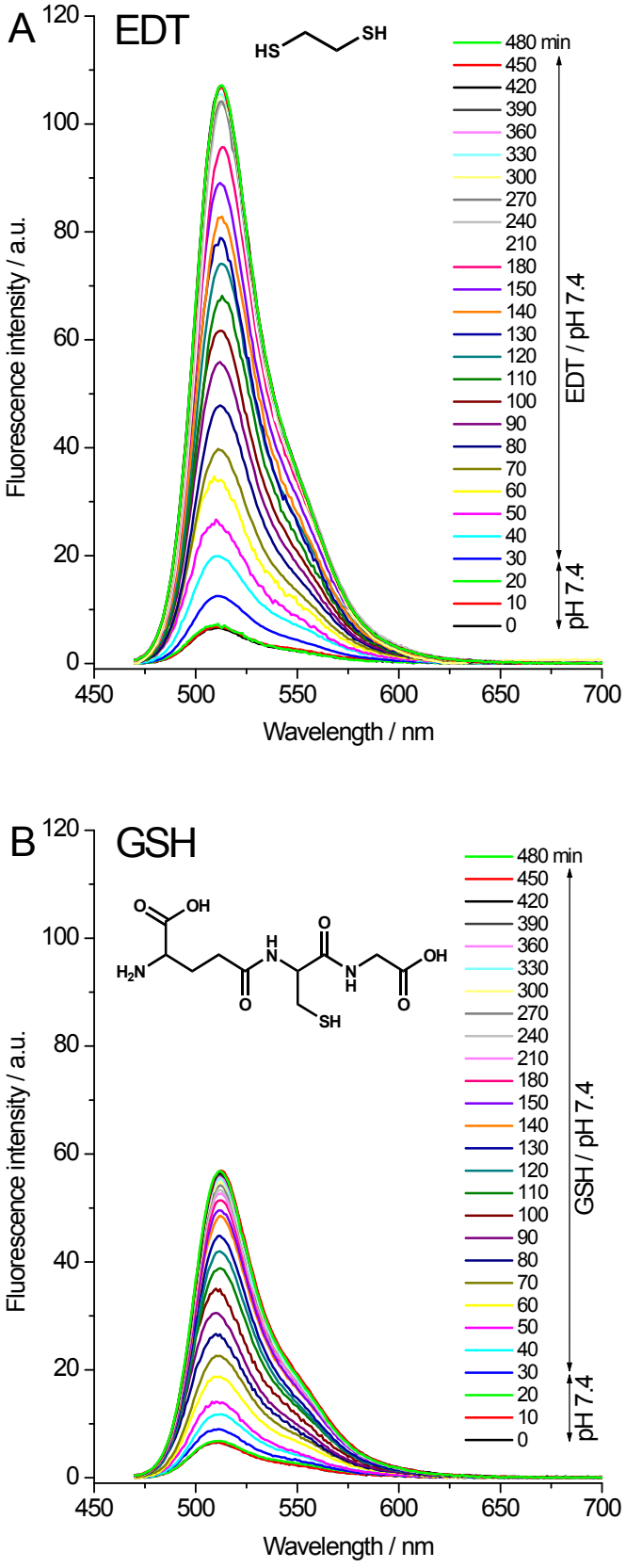

Fig. S24 Fluorescence spectra of calcein (λ_{ex} = 458 nm, λ_{em} = 510 nm) released from γ-CD-gated MSNs only with the loading of calcein in the MSN pores upon addition of triggers at pH 7.4 after 30 min: (A) EDT (5 mM); (B) GSH (5 mM); (c) BDO (10 mM).

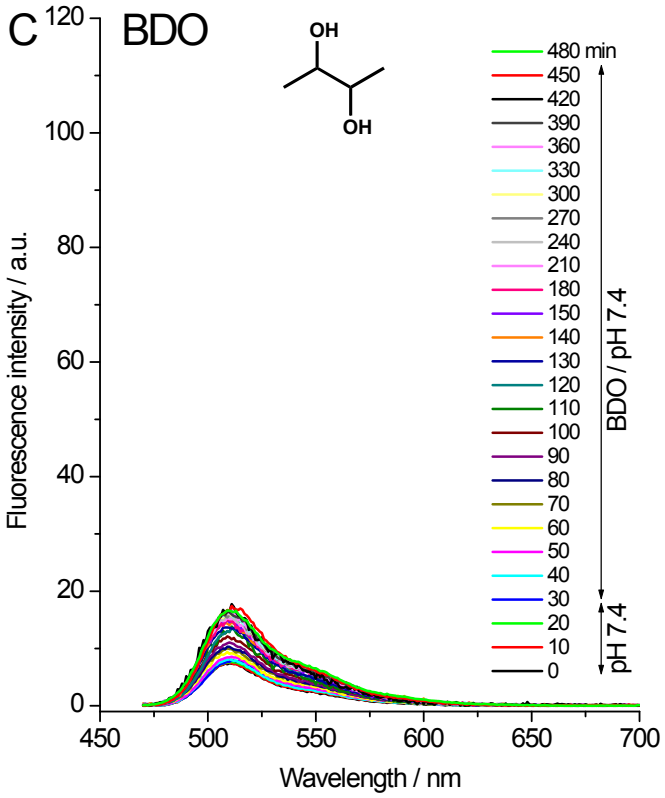

Fig. S24 (continuted)

To confirm whether the cargo release from the MSN pores resulted from the cleavage of the disulfide bonds by the mercapto groups or from the competitive binding of the diols to the PBA moieties, 2,3-butanediol (BDO) and 1,2-ethanedithiol (EDT) were selected as potential triggers for comparison (Fig. 4A and Fig. S24). BDO only gave rise to very little release even at the concentration 10 mM with respect to the case before trigger, while EDT (5 mM) caused significant cargo release similar to DTT (5 mM) with an identical release profile. These comparative experiments demonstrate that **the DTT-responsive controlled release of calcein resulted from the cleavage of the disulfide bonds**.

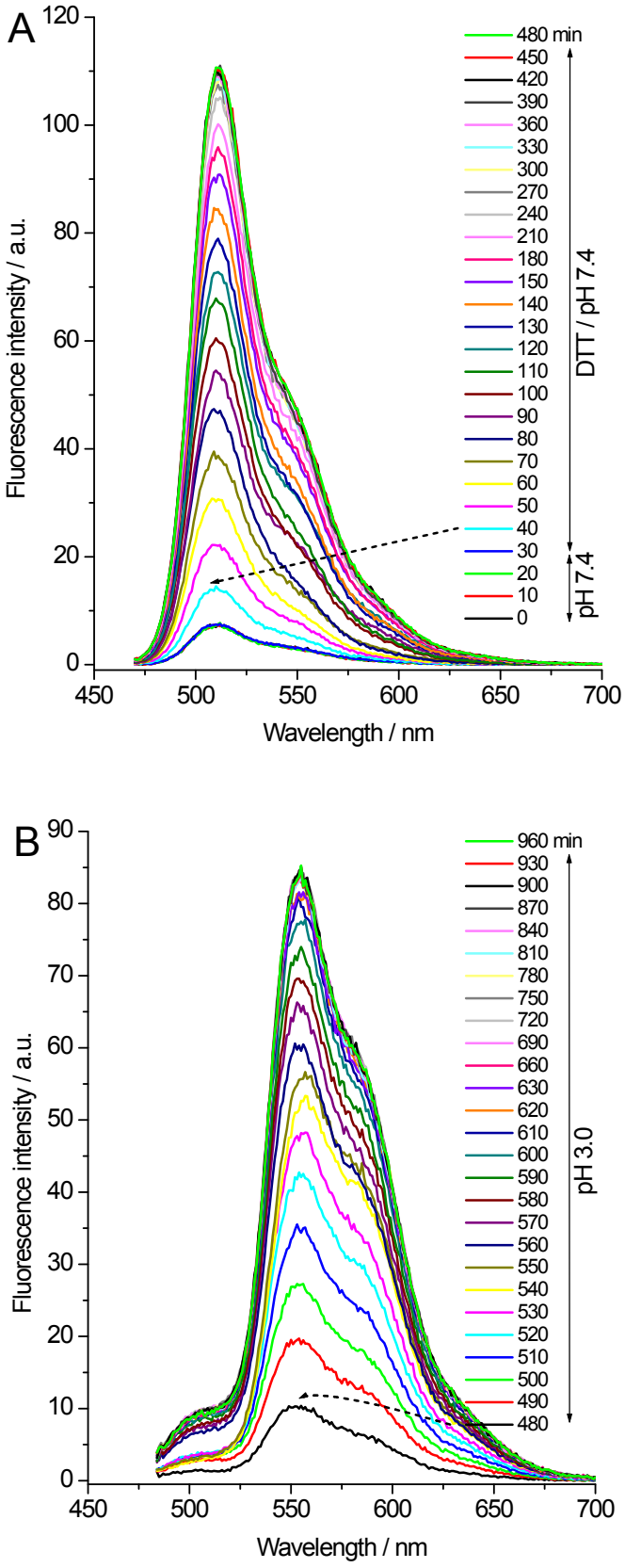

Fig. S25 Fluorescence spectra of drugs released from γ-CD-gated MSNs with dual loading of calcein and DOX upon first trigger of DTT (5 mM) at pH 7.4 after 30 min and subsequent trigger of pH 3.0 after 480 min: (A) calcein (λ_{ex} = 458 nm, λ_{em} = 510 nm); (B) DOX (λ_{ex} = 480 nm, λ_{em} = 555 nm).

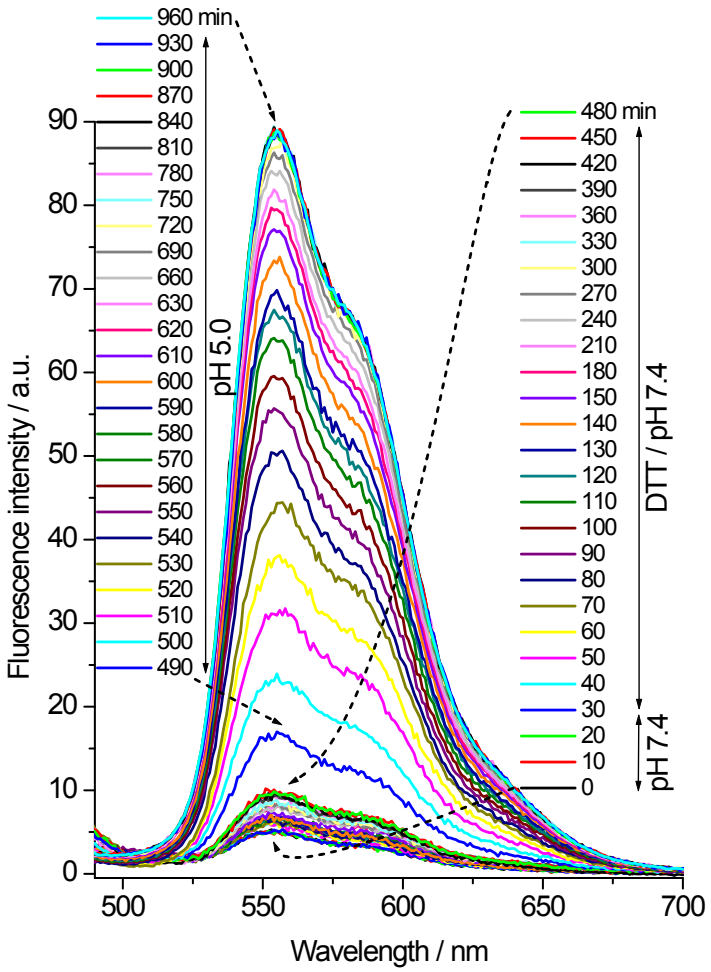

Fig. S26 Fluorescence spectra of DOX (λ_{ex} = 480 nm, λ_{em} = 555 nm) released from γ-CD-gated MSNs only with the loading of DOX inside the γ-CD cavities upon first trigger of DTT (5 mM) at pH 7.4 after 30 min and subsequent trigger of pH 5.0 after 480 min.

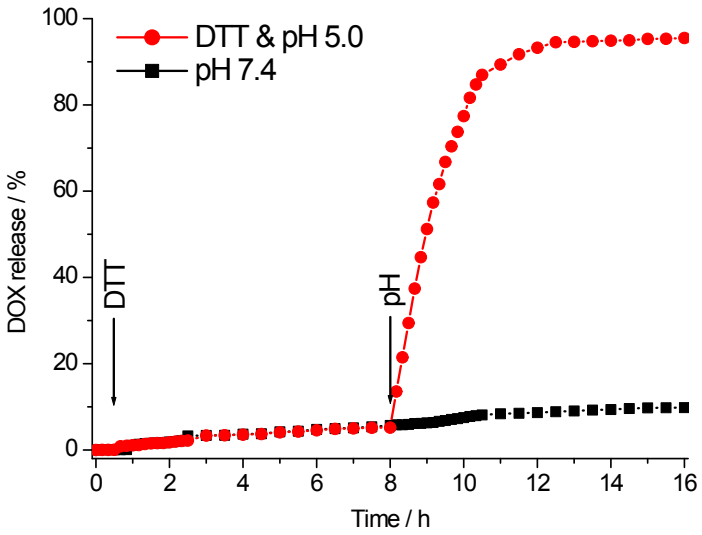

Fig. S27 Release profile of DOX from γ-CD-gated MSNs only with the loading of DOX inside the γ-CD cavities upon first trigger of DTT (5 mM) at pH 7.4 and subsequent trigger of pH 5.0 in comparison to the case at pH 7.4 without trigger: DOX (λ_{ex} = 480 nm, λ_{em} = 555 nm).

To gain insight into the probable influence of fluorescence emission of calcein on that of DOX, the γ-CD-gated MSNs only with loading of DOX inside the γ-CD cavities (no cargo within the MSN pores) were studied for comparison (Fig. S26 and S27). The addition of DTT could not give rise to the release of DOX, but acidic pH triggered the DOX release. It is obvious that the first release of calcein almost had no influence on monitoring of subsequent release of DOX. These results further demonstrate the cascade release of the two drugs under the successive triggers.

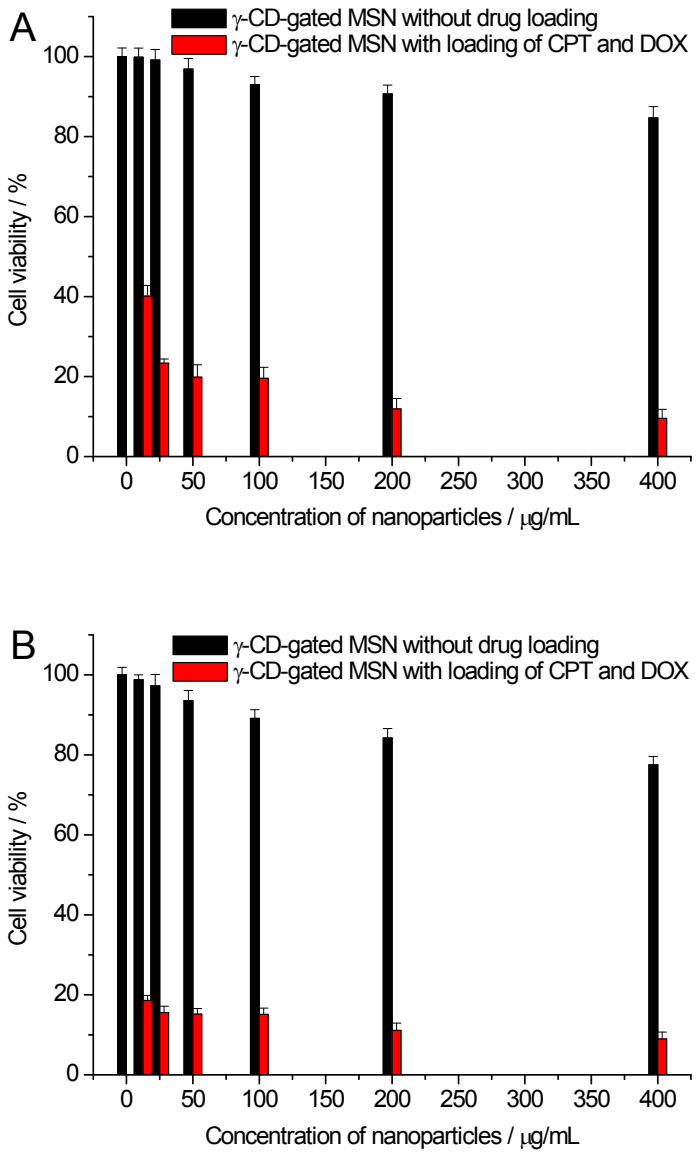

Fig. S28 In vitro cytotoxicity of γ-CD-gated MSNs with and without dual loading of CPT and DOX incubated with cells for 24 h: (A) HeLa cells; (B) A549 cells.

HeLa cells were incubated with the γ-CD-gated MSNs with dual drug loading to examine acidic pH-triggered drug release. The cytotoxicity of the γ-CD-gated MSNs with and without dual drug loading was evaluated by the MTT assay. The γ-CD-gated MSNs without drug loading showed a low cytotoxicity after 24 h of incubation, however, the γ-CD-gated MSNs with dual drug loading showed antiproliferative activity against HeLa cells with the cell viability of less than 10% (Fig. S28A). Furthermore, A549 cells cells were incubated with the γ-CD-gated MSNs with dual drug loading. There are high GSH levels within A549 cells besides weak acidic environments. The γ-CD-gated MSNs with dual drug loading showed lower cell viabilities in the case of A549 cells than those in the case of HeLa cells, especially at the low dosages of the nanoparticles (Fig. S28B). **The very low cell viabilities were attributed to the simultaneous/cascade release and synergistic effect of the two drugs triggered by acidic pH and GSH.**